The operators $a(\mathbf{p})$ and $b(\mathbf{p})$ satisfy

$$[a(\mathbf{p}),a^\dagger(\mathbf{p}')]=[b(\mathbf{p}),b^\dagger(\mathbf{p}')]=\delta(\mathbf{p}-\mathbf{p}'),$$

all other commutators vanishing.

The energy-momentum and charge operators are

$$P^\mu=\int[a^\dagger(\mathbf{p})a(\mathbf{p})+b^\dagger(\mathbf{p})b(\mathbf{p})]p^\mu d^3p,$$

$$Q=e\int[b^\dagger(\mathbf{p})b(\mathbf{p})-a^\dagger(\mathbf{p})a(\mathbf{p})]d^3p,$$

where e is the charge of the positron. Thus $a(\mathbf{p})$ and $b(\mathbf{p})$ annihilate negatively charged and positively charged mesons, respectively.

For the neutral π-meson field, we impose the restriction $\psi=\psi^C$ and take for our Lagrangian density

$$L=-\tfrac{1}{2}i\bar{\psi}(\partial_\mu\beta^\mu-im)\psi. \qquad \text{(A7)}$$

The commutation relations are[20]

$$[\psi_a(x),\psi_b(x')]=-[R(x-x')C^*\bar{\eta}^0]_{ab},$$

and the Fourier expansion becomes

$$\psi(x)=(2\pi)^{-\frac{3}{2}}\int d^3p[c(\mathbf{p})u(\mathbf{p})e^{-ip\cdot x}-c^\dagger(\mathbf{p})v(\mathbf{p})e^{ip\cdot x}],$$

where $[c(\mathbf{p}),c^\dagger(\mathbf{p}')]=\delta(\mathbf{p}-\mathbf{p}')$ and

$$[c(\mathbf{p}),c(\mathbf{p}')]=[c^\dagger(\mathbf{p}),c^\dagger(\mathbf{p}')]=0.$$

The energy-momentum operator for neutral pions is

$$P^\mu=\int c^\dagger(\mathbf{p})c(\mathbf{p})p^\mu d^3p.$$

The Kemmer Eq. for spin one-half particles has been discussed elsewhere.[21]

[20] Because of the form of the generator obtained from (A7), care must be taken with regard to a factor of $\frac{1}{2}$ when deriving the canonical commutation relations. See, for example, J. Schwinger, Phil. Mag. 44, 1171 (1953).

[21] A. O. Barut, M. Samiullah, Nuovo cimento 17, 876 (1960).

PHYSICAL REVIEW VOLUME 121, NUMBER 3 FEBRUARY 1, 1961

Spin-Momentum Correlations in Positron-Electron Scattering

C. FRONSDAL* AND B. JAKŠIĆ†
CERN, Geneva, Switzerland

(Received September 27, 1960)

The imaginary part of the fourth-order Bhabha (e^+-e^-) scattering matrix element interferes with the (real) second-order matrix element, to produce a sixth-order dependence of the cross section on the spin of one of the particles (after summing over the spins of the other three particles). The process of extracting the imaginary part of the fourth-order matrix element is presented in some detail in one of the graphs (vacuum polarization).

I

SPIN-MOMENTUM correlations in the scattering of electrons by atomic nuclei (Mott scattering) are well known. Until recently, however, effects of this kind have not been studied in the scattering of leptons by leptons. Calculations have been performed by $\mu-e$ and e^-e^- scattering, and the results found to be very small.[1] Because of the qualitative difference between this case and that of Bhabha (e^+-e^-) scattering, due to the existence of annihilation graphs, it was thought that the effect might be more important in the latter process. In the present paper, results for Bhabha scattering are presented. These are also found to be small.

In reference 1, the imaginary part of the fourth-order scattering matrix element was calculated by using unitarity. We have therefore chosen to give a short exposition of an alternative method. The imaginary part is here extracted from the complete fourth-order matrix element. (See Fig. 1.) After performing two trivial contour integrations the imaginary part is easily isolated. The remaining (angular) integrations are performed *after* the trace calculations.

As was pointed out in reference 1, diagrams of the type of Fig. 2 do not contribute to the spin-momentum correlations. Arguments for the neglect of rescattering by the nucleus (valid for scattering by hydrogen) were also given there.

II

If the positron beam (particle 2, momentum p_2) is partly polarized, with degree of polarization ξ, then the cross section may be written

$$\sigma=\sigma_0(1+\xi P), \qquad (1)$$

* Present address, University of Pennsylvania, Philadelphia 4, Pennsylvania.
† Present address, Institut Ruder Bošković, Zagreb, Jugoslavija.

[1] A. Barut and C. Fronsdal, Phys. Rev. **120**, 1871 (1960).

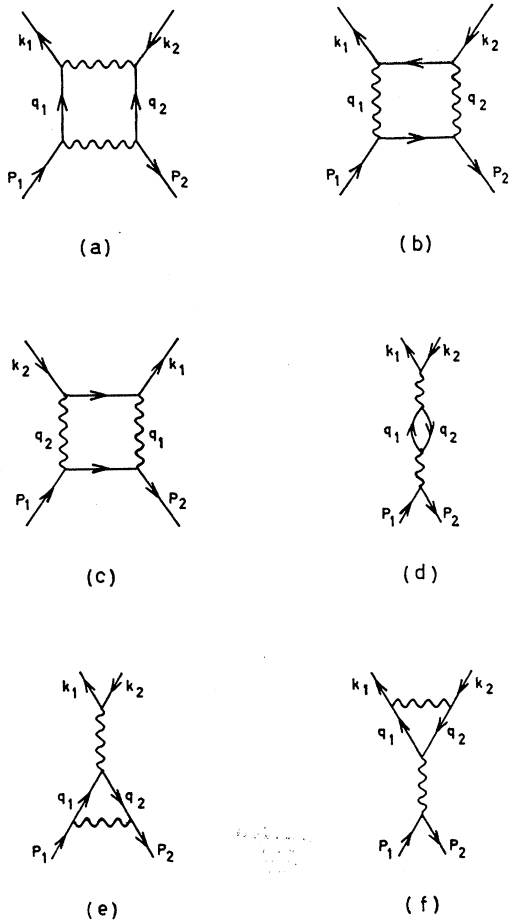

FIG. 1. In fourth-order Bhabha scattering these diagrams have imaginary parts, since every one of them can be cut by a horizontal line such that each half represents a real physical process.

where σ_0 is the ordinary Bhabha differential cross section, and

$$P=\mathrm{tr}\{M^\dagger\boldsymbol{\sigma}\cdot\mathbf{s}M\}/\mathrm{tr}\{M^\dagger M\}.$$

The matrix element M is defined by

$$S=1+iM\equiv 1+iM_2+iM_4+\cdots.$$

In the laboratory system, as well as in the center-of-mass system, only the transverse component of $\mathbf{s}$ contributes to P. Since P vanishes for Hermitian or anti-Hermitian M, and because $\mathrm{Im}M_2=0$, we have to lowest nonvanishing order

$$P=2i\ \mathrm{tr}\{M_2^\dagger\boldsymbol{\sigma}\cdot\mathbf{s}\ \mathrm{Im}M_4\}/\mathrm{tr}\{M_2^\dagger M_2\}. \quad (2)$$

FIG. 2. Diagrams such as this one are important in sixth-order cross-section calculations, since they serve to eliminate the infrared divergences. These diagrams have no imaginary parts, however, and hence do not contribute to the spin-momentum correlations. Our calculation, which is based on the diagrams of Fig. 1 only, must therefore give a finite result.

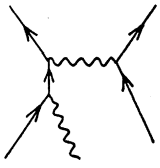

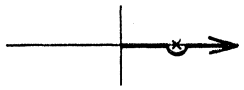

FIG. 3. The contour of the integration over $\mathbf{q}^2$ in the complex $\mathbf{q}^2$ plane. Only the integral around the infinitesimal semicircle contributes to the imaginary part.

In order to illustrate the calculation of $\mathrm{Im}M_4$, consider the graph of Fig. 1(d). The corresponding part of M_4 is (we calculate in the center-of-mass system):

$$M_4^{(d)}=e^4(2\pi)^{-6}\frac{m^2}{E^2}i\int\frac{d^4q_1}{(p_1-p_2)^4}\times\bar\psi(p_2)\gamma_\mu\psi(p_1)\bar\psi(k_1)\gamma_\nu\psi(k_2)\times\mathrm{tr}\{(\mathbf{q}_2-im)^{-1}\gamma_\nu(\mathbf{q}_1-im)^{-1}\gamma_\mu\}. \quad (3)$$

Writing $q_1=(iQ,\mathbf{q})$, $q_2=(-2iE+iQ,\mathbf{q})$, we have $d^4q_1=d^3\mathbf{q}dQ$. The integrand has four poles in the Q-complex plane. Following Feynman's prescription we displace these off the real axis, so that they are located at

$$Q=Q_\pm^{(1)}\equiv\pm(m^2+\mathbf{q}^2)^{\frac{1}{2}}\mp i\epsilon,$$

and

$$Q=Q_\pm^{(2)}\equiv 2E\pm(m^2+\mathbf{q}^2)^{\frac{1}{2}}\mp i\epsilon.$$

The integral over Q, running along the real axis from $-\infty$ to $+\infty$, equals $2\pi i$ times the sum of the residues of the two poles in the upper half plane. These residues have poles at some points in the complex $\mathbf{q}^2$ plane. Thus the residue of the pole at $Q_-^{(2)}$ contains the factor

$$[(Q_-^{(2)}-Q_+^{(2)})(Q_-^{(2)}-Q_+^{(1)})(Q_-^{(2)}-Q_-^{(1)})]^{-1}. \quad (4)$$

In the limit $\epsilon\to 0$, the term $Q_-^{(2)}-Q_+^{(1)}$ gives a pole for real[2] $\mathbf{q}$ at $\mathbf{q}^2=E^2-m^2\equiv p^2$, and the contour of the $\mathbf{q}^2$ integration is shown in Fig. 3. The separation of M_4 into its real and imaginary parts is therefore displayed by the formula

$$\lim_{\epsilon\to 0}(Q_-^{(2)}-Q_+^{(1)})^{-1}=P(Q_-^{(2)}-Q_+^{(1)})^{-1}+\pi i\delta(Q_-^{(2)}-Q_+^{(1)}). \quad (5)$$

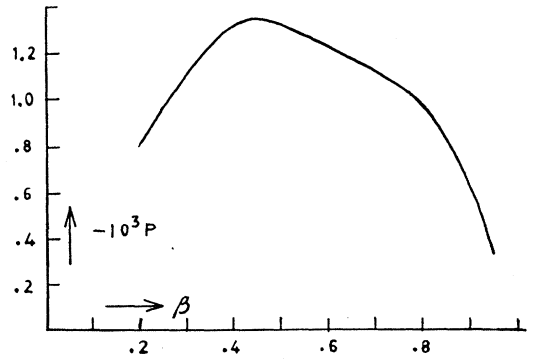

FIG. 4. A plot of $P(\beta,\vartheta)$ as given by (8), in the case that the spin $\mathbf{s}$ is parallel to $\mathbf{p}_1\times\mathbf{k}_1$ [that is, the second factor in (8) is set equal to unity]. The abscissa is the center-of-mass velocity β, and ϑ is the center-of-mass scattering angle. The value $\vartheta=120°$ is near the maximum of Fig. 5.

[2] The residue of the pole at $Q_-^{(1)}$ does not have a pole for real $\mathbf{q}$.

Hence we obtain, after essentially no calculation,

$$\mathrm{Im}M_4^{(d)}=e^4(2\pi)^{-6}\frac{m^2}{E^2}\left(-\frac{\pi^2}{4}\frac{p}{E}\right)\int\frac{d\Omega}{(p_1-p_2)^4}$$
$$\times\bar\psi(p_2)\gamma_\mu\psi(p_1)\bar\psi(k_1)\gamma_\nu\psi(k_2)$$
$$\times\mathrm{tr}\{(\mathbf{q}_2+im)\gamma_\nu(\mathbf{q}_1+im)\gamma_\mu\},\quad(6)$$

where $q_1=(iE,\mathbf{q})$, $q_2=(-iE,\mathbf{q})$, $\mathbf{q}^2=p^2$, and the integral is over the directions of $\mathbf{q}$.

We saw that the imaginary part of $M_4^{(d)}$ arises from the coincidence, for a real value of $\mathbf{q}$, of two poles in the energy plane, and that this coincidence occurs when both the intermediate particles are on their mass shells. This is an example of a very general and well-known feature of scattering amplitudes; namely, that an imaginary part exists only when there exists a real intermediate state. In perturbation theory this means the possibility of splitting a diagram in two parts by a space-like surface, in such a way that both halves are the diagrams of real processes in lower order.[3] It is easy to see that of all the fourth-order diagrams for Bhabha scattering, only those of Fig. 1 have this property.

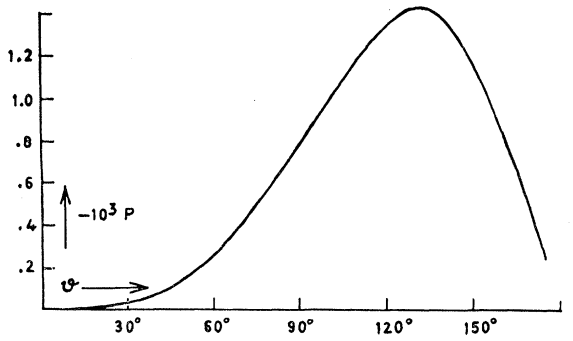

FIG. 5. Same as Fig. 4, except that the abscissa is now ϑ and $\beta=p/E$ has been chosen equal to 0.5 which is near the maximum of Fig. 4.

We have calculated all the imaginary parts by the above method, as well as by unitarity. The results are

$$\mathrm{Im}M_4^{(a)}=-\frac{e^2}{(2\pi)^6}\frac{m^2}{E^2}\frac{\pi^2}{4}\frac{p}{E}\int\frac{d\Omega}{(\mathbf{q}-\mathbf{p}_2)^2(\mathbf{q}-\mathbf{k}_2)^2}\bar\psi(p_2)\gamma_\mu(\mathbf{q}_2+im)\gamma_\nu\psi(k_2)\bar\psi(k_1)\gamma_\nu(\mathbf{q}_1+im)\gamma_\mu\psi(p_1),$$

$$\mathrm{Im}M_4^{(b)}=\frac{e^4}{(2\pi)^6}\frac{m^2}{E^2}\frac{\pi^2}{4}\int d\Omega\bar\psi(k_1)\gamma_\mu(\mathbf{k}_2-\mathbf{q}_2'-im)^{-1}\gamma_\nu\psi(k_2)\bar\psi(p_2)\gamma_\nu(\mathbf{p}_2-\mathbf{q}_2'-im)^{-1}\gamma_\mu\psi(p_1),$$

$$\mathrm{Im}M_4^{(c)}=\frac{e^4}{(2\pi)^6}\frac{m^2}{E^2}\frac{\pi^2}{4}\int d\Omega\bar\psi(k_1)\gamma_\mu(\mathbf{k}_2-\mathbf{q}_2'-im)^{-1}\gamma_\nu\psi(k_2)\bar\psi(p_2)\gamma_\mu(\mathbf{p}_1+\mathbf{q}_2'-im)^{-1}\gamma_\nu\psi(p_1),\quad(7)$$

$$\mathrm{Im}M_4^{(e)}=\frac{e^4}{(2\pi)^6}\frac{m^2}{E^2}\frac{\pi^2}{4}\frac{p}{E}\int\frac{d\Omega}{4E^2(\mathbf{q}-\mathbf{p}_2)^2}\bar\psi(k_1)\gamma_\mu\psi(k_2)\bar\psi(p_2)\gamma_\nu(\mathbf{q}_2+im)\gamma_\mu(\mathbf{q}_1+im)\gamma_\nu\psi(p_1),$$

$$\mathrm{Im}M_4^{(f)}=\frac{e^4}{(2\pi)^6}\frac{m^2}{E^2}\frac{\pi^2}{4}\frac{p}{E}\int\frac{d\Omega}{4E^2(\mathbf{q}-\mathbf{k}_2)^2}\bar\psi(k_1)\gamma_\mu(\mathbf{q}_1+im)\gamma_\nu(\mathbf{q}_2+im)\gamma_\mu\psi(k_2)\bar\psi(p_2)\gamma_\nu\psi(p_1),$$

$$q_{10}=-q_{20}=-q_{20}'=E,\quad\mathbf{q}_1^2=\mathbf{q}_2^2=p^2,\quad\mathbf{q}_2'^2=E^2.$$

We insert this result into Eq. (2), evaluate first the traces and then the angular integrals. A small photon mass λ is introduced in order to evaluate the logarithmic divergences, letting λ tend to zero at the end. The divergences cancel. (See Fig. 1.) The result is

$$P=\frac{(1-\beta^2)^{\frac{1}{2}}}{137\beta\sin\vartheta}\frac{\mathbf{s}\cdot\mathbf{p}_1\times\mathbf{k}_1}{|\mathbf{p}_1\times\mathbf{k}_1|}\frac{A}{B},\quad(8)$$

[3] See, e.g., R. J. Eden, Proc. Roy. Soc. (London) **A210**, 388 (1952).

where **s** is the direction of the spin of the physical positron (rather than that of the hole), and

$$\beta=p/E,\quad x=\sin(\vartheta/2),$$

$$A=\frac{3}{\beta^2}[1-3\beta^2-2\beta^4(1-x^2)]\ln x^2+\frac{4}{\beta}(1-x^2)(2x^2\beta^2-1)+2(1-x^2)[1-\beta^2(10+3x^2)+\beta^4(1-x^2+2x^4)]$$
$$+\frac{1}{\beta^2x^2}[-3+5x^2-2x^4+\beta^2(-3+10x^2-2x^4+4x^6)-\beta^4x^2(3-4x^2+4x^4)]\ln\frac{1+\beta}{1-\beta}$$
$$+\frac{6\beta}{1-\beta^2}[2-5x^2+\beta^2(-2+7x^2-4x^4)]L\left(\frac{\beta x}{(1-\beta^2)^{\frac{1}{2}}}\right)$$
$$+\frac{1-x^2}{x^2}\frac{6\beta}{1-\beta^2}\left[2-5x^2+\beta^2x^2(-1+4x^2)+\frac{1-\beta^2}{\beta^2}\right]L\left(\frac{\beta(1-x^2)^{\frac{1}{2}}}{(1-\beta^2)^{\frac{1}{2}}}\right),$$

$$B=\frac{1}{\beta^4}\frac{1}{x^4}+\frac{1}{\beta^2}\left(\frac{2}{x^4}-\frac{7}{x^2}\right)+\frac{1}{x^4}-\frac{2}{x^2}+13+\beta^2\left(\frac{1}{x^2}-2-4x^2\right)+\beta^4(1-2x^2)^2,$$

$$L(z)=z^{-1}(1+z^2)^{-\frac{1}{2}}\operatorname{arcsinh}z.$$

III

Numerical results are given in Figs. 4, 5, 6, and 7. In Fig. 4 is plotted $P(\beta,\vartheta)$ for **s** parallel to $\mathbf{p}_1\times\mathbf{k}_1$, $\vartheta=120°$, $0<\beta<1$ and shows a maximum near $\beta=0.5$. In Fig. 5 is plotted $P(\beta,\vartheta)$ for **s** parallel to $\mathbf{p}_1\times\mathbf{k}_1$, $\beta=0.5$, $0<\vartheta<180°$, and shows a maximum near $\vartheta=120°$. In Figs. 6 and 7 are shown the second-order cross sections for the same parameter values. The numerical values of P are of the same order of magnitude as for Møller scattering.[1]

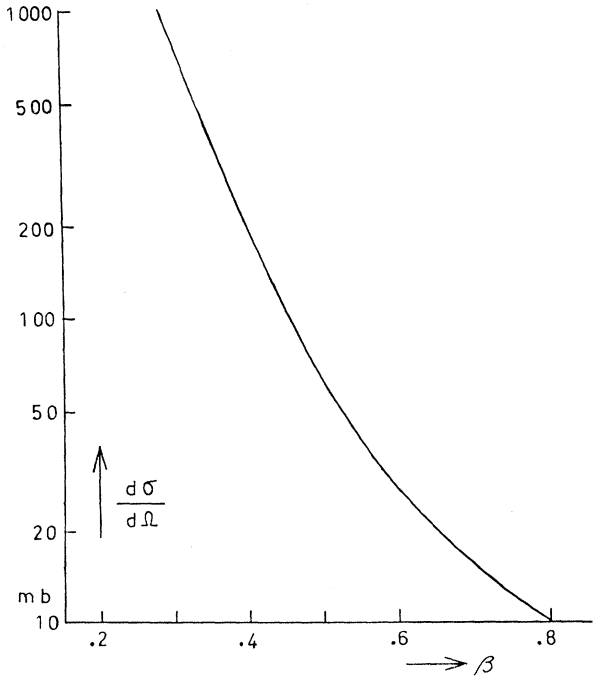

FIG. 6. A plot of the total second-order Bhabha scattering cross section with the same parameter values as in Fig. 4.

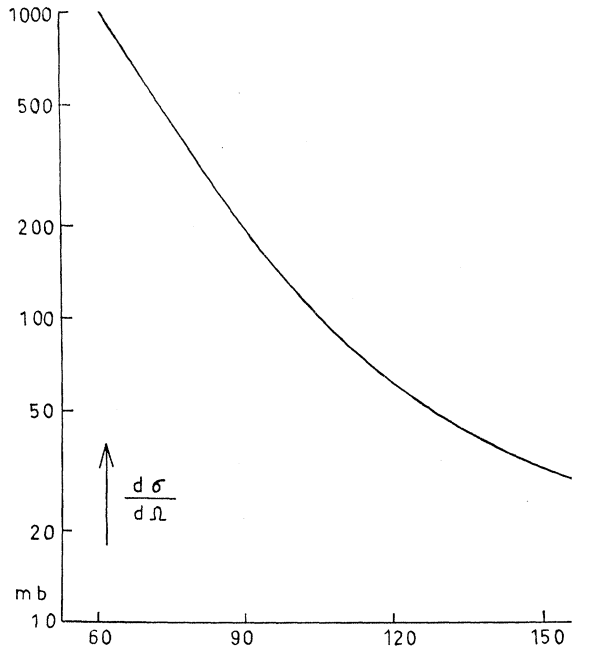

FIG. 7. A plot of the total second-order Bhabha scattering cross section with the same parameter values as in Fig. 5.

ACKNOWLEDGMENTS

We are grateful to Professor V. Telegdi for reminding us of the importance of rescattering by the nucleus in the case of heavy nuclei, and to Professor M. Fierz and many other members of the CERN Theoretical Study Group for interesting discussions. Our special thanks to Professor Fierz and Professor Bakker for the hospitality extended to us at CERN.